https://doi.org/10.5194/gmd-2021-330
Preprint. Discussion started: 3 December 2021

Geoscientific Model Development Discussions

Towards an improved representation of carbonaceous aerosols over the Indian monsoon region in a regional climate model RegCM4.6

Sudipta Ghosh[1], *Sagnik Dey[1,2], Sushant Das[3], Nicole Riemer[4], Graziano Giuliani[3], Dilip Ganguly[1], Chandra Venkatraman[5], Filippo Giorgi[3], Sachchida Nand Tripathi[6], Ramachandran Srikanthan[7], Rajesh Ayyappen Thazhathakal[7], Harish Gadhavi[7], Atul Kumar Srivastava[8]

[1]Centre for Atmospheric Sciences, Indian Institute of Technology Delhi, India
[2]Centre of Excellence for Research on Clean Air, Indian Institute of Technology Delhi, India
[3]Earth System Physics Section, ICTP, Trieste, Italy
[4]Department of Atmospheric Sciences, University of Illinois at Urbana-Champaign, IL, USA
[5]Department of Chemical Engineering, Indian Institute of Technology Bombay, India
[6]Department of Civil Engineering, Indian Institute of Technology Kanpur, India
[7]Space and Atmospheric Sciences Division, Physical Research Laboratory, Ahmedabad, India
[8]Indian Institute of Tropical Meteorology, New Delhi, India

***Correspondence: sagnik@cas.iitd.ac.in**

Keywords: RegCM4; emission inventory; carbonaceous aerosols; model customization; Indian monsoon region

Abstract

Mitigation of carbonaceous aerosol emissions is expected to provide climate and health co-benefits. The accurate representation of carbonaceous aerosols in climate models is critical for reducing uncertainties in their climate feedbacks. In this regard, emission fluxes and aerosol life-cycle processes are the two primary sources of uncertainties. Here we demonstrate that incorporating a dynamic ageing scheme and emission estimates that are updated for the local sources improve the representation of carbonaceous aerosols over the Indian monsoon region in a regional climate model, RegCM, compared to its default configuration. The mean BC and OC surface concentrations in 2010 are estimated to be 4.25 and 10.35 μg m^{-3}, respectively, over the Indo-Gangetic Plain (IGP), in the augmented model. The BC column burden over the polluted IGP is found to be 2.47 mg m^{-2}, 69.95% higher than in the default model configuration and much closer to available observations. The anthropogenic AOD increases by more than

https://doi.org/10.5194/gmd-2021-330
Preprint. Discussion started: 3 December 2021


Geoscientific Model Development Discussions

19% over the IGP due to the model enhancement, also leading to a better agreement with observed AOD. The top-of-the-atmosphere, surface, and atmospheric anthropogenic aerosol shortwave radiative forcing are estimated at -0.3, -9.3, and 9.0 W m^{-2}, respectively, over the IGP and -0.89, -5.33, and 4.44 W m^{-2}, respectively, over Peninsular India. Our results suggest that both the accurate estimates of emission fluxes and a better representation of aerosol processes are required to improve the aerosol life cycle representation in the climate model.

1. Introduction

Carbonaceous aerosols (organic carbon, OC, and black carbon, BC) emitted from incomplete combustion constitute 20%-50% of the total global aerosol mass (Kanakidou et al., 2005; Putaud et al., 2010), causing substantial air quality degradation (Singh et al., 2021). Due to their ability to absorb solar radiation, carbonaceous aerosols also contribute to global warming (Ramanathan and Carmichael, 2008). Hence, they are considered to be key short-lived climate pollutants (SLCPs) (UNFCC, 2015), and mitigating their emissions is expected to result in both climate and health co-benefits (Tibrewal and Venkataraman, 2021). Climate models are characterized by large discrepancies in simulating carbonaceous aerosol loadings, their optical properties, and radiative forcing (Ajay et al., 2019), primarily due to uncertainties in emission inventories and limitations in the treatment of aerosol processes in the models (Bond et al., 2013). Unless the representation of the life cycle of carbonaceous aerosols in climate models is improved, their role in climate impacts and air quality degradation cannot be assessed accurately (Riemer et al., 2019).

A multi-institutional network program - Carbonaceous aerosol emissions, source apportionment, and climate impacts (COALESCE) was launched by the Government of India to address some of these issues for the Indian monsoon region (Venkataraman et al., 2020). One of the scientific objectives of COALESCE is to understand and reduce uncertainties in representing carbonaceous aerosol life cycle in global and regional climate models, focusing on the Indian subcontinent. The regional climate model, RegCM4, developed at the International Centre for Theoretical Physics (ICTP), Italy (Giorgi et al., 2012), is one of the participating models in COALESCE. RegCM4 was extensively used to examine variability in the Indian summer monsoon (Dash et al., 2006; Rai et al., 2019), to project climate change over South Asia (Pattanayak et al., 2019), and to elucidate the dynamical impacts of aerosols on the Indian summer monsoon in the present (Das et al., 2015; 2016) and future (Das et al., 2020) climate conditions.

https://doi.org/10.5194/gmd-2021-330
Preprint. Discussion started: 3 December 2021


Geoscientific Model Development Discussions

The aerosol module in the RegCM4 (Solmon et al., 2006; Zakey et al., 2006) considers various aerosol life cycle processes, such as emission (source), advection, horizontal and vertical diffusion, transport, conversion of hydrophobic to hygroscopic species, and wet and dry deposition (sink). Previous studies (Das et al., 2016) have pointed out that the RegCM4 underestimates the anthropogenic aerosol loading over the Indian subcontinent, and therefore, the net aerosol impact over the region is dominated by natural aerosols (Das et al., 2020). We recently implemented a dynamic ageing scheme in the RegCM aerosol module (Ghosh et al., 2021), which converts carbonaceous aerosols from hydrophobic to hygroscopic states based on the aerosol number concentration. Compared to the constant conversion rate of 27.6 hours used in the default version of the model, the scheme allowed a faster conversion in the polluted regions than in the clean areas of the South Asia region. This, in turn, affected the aerosol forcing due to the changes in aerosol loadings induced by the new hydrophobic-to-hygroscopic conversion scheme. It was also found that implementing the dynamic ageing scheme alone is not sufficient to fully improve the model performance and hypothesized that much of the model uncertainty was due to the emission inventory.

In this work, we examine the changes in carbonaceous aerosol burden and their impact on the radiation budget over the South Asia region due to the combined impact of the new dynamic ageing scheme and a regional emission inventory (Venkataraman et al., 2018) replacing the global emission inventory used in the default model version. We carry out four sets of simulations for the year 2010 - (1) control simulation with the default (fixed) ageing scheme and global inventory (hereafter Default_Sc), (2) simulation with the dynamic ageing scheme and global inventory (Dyn_global), (3) simulation with the default ageing scheme and regional inventory (Fix_Regio) and (4) simulation with the dynamic ageing scheme and regional emission inventory (Dyn_Regio). We analyse and report the improvements in model performance due to the combined impact of incorporating a better emission inventory and a more realistic ageing scheme relative to the default model configuration and investigate these performance changes in terms of the aerosol processes considered in the model.

2. Data and Methodology

2.1 Model configuration

In this work, we have used a regional climate model, RegCM version 4. It is a compressible, hydrostatic, and primitive equation model with a sigma-p vertical coordinate and a dynamical core from the NCAR Mesoscale Model Version 5 (MM5)(Grell, 1993). We have used the Community Climate Model Version 3 (CCM3)(Kiehl et al., 1996) radiative transfer scheme along with the changes mentioned in the literature (Giorgi et al., 2012). Interactive modules for

https://doi.org/10.5194/gmd-2021-330
Preprint. Discussion started: 3 December 2021


Geoscientific Model Development Discussions

101 both natural (dust and sea salt) (Zakey et al., 2006, 2008) and anthropogenic aerosols (Solmon
102 et al., 2006) are integrated into RegCM4. The model is also coupled with a gas-phase chemistry
103 module (Shalaby et al., 2012); however, for the current study, we have only considered the
104 anthropogenic module (Solmon et al., 2006). The choice of parameterisation schemes for our
105 experiments have been provided in the following table:
106

Land surface processes	Biosphere-Atmosphere Transfer Scheme (BATS) (Dickinson et al., 1993)
Planetary boundary layer	University of Washington (UW) scheme (Grenier and Bretherton, 2001; Bretherton et al., 2004; O'Brien et al., 2012)
Cumulus convection scheme	Emanuel (Emanuel and Rothman, 1999) over land and Tiedtke (Tiedtke, 1989) over the ocean
Large scale cloud and moisture process	SUBEX scheme (Pal et al., 2000)
Aerosol module	SUCA (Solmon et al., 2006)
Emission inventories	IIASA and IIT Bombay 2010

107

108 The model was simulated over the South-Asian CORDEX domain (Giorgi et al., 2009) [20°
109 S - 50° N and 10°-130° E] for the year 2010 at 0.25° × 0.25° resolution, while the results are
110 analysed over the Indian subcontinent [5°- 40° N and 65°-100° E] with special focus on the
111 IGP [Figure 1] and PI [8° - 20° N and 72° - 85° E]. The simulations consist of 18 vertical levels
112 with the model top pressure at 50 hPa. ERA-Interim 6-hourly reanalysis dataset, at 1.5°
113 resolution, has been used to generate the initial and lateral meteorological boundary conditions
114 for this study (Dee et al., 2011). The sea surface temperature was derived from the NOAA
115 Optimum Interpolated weekly 1° × 1° gridded data and the chemical boundary conditions from
116 MOZART 6-hourly data. The model was simulated from October 01, 2009, to December 31,
117 2010. The first three months are considered as spin-up and thus are not included in the analysis.
118 Aerosol atmospheric lifetime is governed by dry and wet deposition. The dry deposition
119 velocity depends on the type of surface, while the dry deposition flux variation varies directly
120 with the tracer concentration at the lowest level of the model (around 30 m above the surface).
121 Wet deposition in the RegCM4 is governed by the "in-cloud" and "below-cloud" terms. When
122 the liquid water content exceeds the threshold level (0.01 g m^{-3}) of the model layers where the

https://doi.org/10.5194/gmd-2021-330
Preprint. Discussion started: 3 December 2021

cloud fraction is more than zero, the in-cloud removal process starts for large-scale clouds. This is then expressed as a function of the fractional removal rate of liquid water (i.e., ratio of precipitating rain over the atmospheric layer liquid water content) and the aerosol solubility. The in-cloud removal rate in RegCM4 for cumulus clouds is fixed at 0.001 s^{-1}) while the aerosol solubility differs with the species variants. Thus the in-cloud wet deposition rates for hydrophilic and hydrophobic BC and OC are different. The below-cloud aerosol wet removal is influenced by their respective effective diameters and densities. Aerosol effective diameter and density, which are different for different species, are used to calculate the collection efficiency for individual aerosol species.

2.2 Implementation of a dynamic ageing parameterisation (Ghosh et al. 2021)

The anthropogenic aerosol module in RegCM4 consists of sulphate, hydrophilic and hydrophobic BC, and hydrophilic and hydrophobic OC. The sulphate scheme has been adapted from Qian et al. (2001). These species are considered as externally mixed while tracking their mass concentrations. During simulations, RegCM4 considers emitted carbonaceous aerosols to be 80% hydrophobic and 20% hydrophilic for BC and equal proportions of hydrophobic and hydrophilic OC. The rate of change of mass mixing ratios of hydrophobic and hydrophilic tracers has been described by the chemical transport equation in Solomon et al. [2006].

The time taken by hydrophobic tracers to get converted into hydrophilic tracers is called "ageing". In the default model set-up, ageing is governed by a fixed e-folding time of 1.15 days (27.6 h) (Cooke et al. 1999). In our recently published work (Ghosh et al., 2021) we have replaced this fixed number with a dynamic ageing scheme (equation 1), where the e-folding time (τ_{mix}) changes as a function of coagulation and condensation. The parameterization has been derived by Fierce et al. (2016) using least square regression on the output of the PartMC-MOSAIC model (Riemer et al., 2009; Zaveri et al., 2008).

$$\tau_{mix} = \frac{1}{I_{cond} \cdot k_{cond} + N \cdot k_{coag}} \qquad (1),$$

where I_{cond} is the condensational flux and N is the total number concentration of all the anthropogenic tracers. The detailed calculations of I_{cond} and N in the jargon of RegCM4 have been provided in Ghosh et al. (2021). Constant values, k_{cond} (0.1 nm^{-1}) and k_{coag} (6 x 10^{-6} cm^3 hr^{-1}) have been derived by implementing the least square regression method on the PartMC model output considering the impact of condensation and coagulation separately (Fierce et al. 2016).

Implementation of the new dynamic ageing scheme in RegCM4 resulted in faster conversion of the hydrophobic to hydrophilic BC and OC, particularly over the polluted IGP. This, in turn,

https://doi.org/10.5194/gmd-2021-330
Preprint. Discussion started: 3 December 2021

increased column burden and surface concentrations of the carbonaceous aerosols over the study region in the dry season. On the contrary, it decreased the burden in the wet season due to a more efficient washout (Ghosh et al., 2021) everywhere except the polluted IGP, where precipitation reduced as a result of radiative feedback.

2.3 Emission inventories

In this study, we replace a global emission inventory [https://www.iiasa.ac.at/web/home/research/researchPrograms/air/Global_emissions.html] with a regional emission inventory (Venkataraman et al., 2018). Figure S1 (see the Supplementary Information, SI) represents the seasonal variation of the emissions estimated by the two inventories. The global emission inventory used in the experiments 'Default_Sc' and 'Dyn_global' was developed by the IIASA emission inventory at a resolution of 0.5° × 0.5° [https://www.iiasa.ac.at/web/home/research/researchPrograms/air/Global_emissions.html]. The key emission sectors considered in this inventory are energy, industry, solvent use, transport, domestic combustion, agriculture, open burning of agricultural waste, and waste treatment. The emission estimates were available only at an annual scale with no seasonal variation from 1990-2010.

The regional emission inventory used in experiments ‘Fix_regio’ and ‘Dyn_regio’ was developed and reported by Venkataraman et al. (2018) at a horizontal resolution of 0.25° × 0.25°, that too at a monthly scale. Thus the regional emissions have a profound seasonal variability (Figure S1). The key sectors included in the regional inventory are energy (coal + oil + gas), heavy and light industry, brick production, residential cooking, solid biomass fuel, residential cooking (LPG and kerosene), residential lighting (kerosene lamp), residential water heating, residential space heating, informal industry, agricultural residue burning, on-road gasoline, on-road diesel, railway, agricultural diesel pump, agricultural tractors. Among these sectors, residential water heating, residential space heating, and agricultural residue burning sectors have seasonality in emissions.

2.3 In-situ BC data

In-situ BC data for the year 2010 has been procured from 28 sites to evaluate the model performance. Twenty-one of these sites is part of the Indian Space Research Organization's Aerosol Radiative Forcing over India Network, ARFINET (Babu et al., 2013; Gogoi et al., 2021). This network has been measuring columnar AOD and BC for many years. In addition to the ARFINET, BC concentrations were also measured independently at Kanpur (Tripathi et al., 2005) during the entire 2010 except the monsoon season, Gadanki (Gadhavi et al., 2015;

https://doi.org/10.5194/gmd-2021-330
Preprint. Discussion started: 3 December 2021

Jain et al., 2018), and Delhi (October-December 2010) by individual institutions. In all the sites, BC was measured by an Aethalometer, which measures the amount of attenuation of the light beam passing through the filter where particles get deposited. BC mass concentration is subsequently estimated by the change in optical attenuation given by the rate of BC deposition on the filter tape (Hansen et al., 1984). Dataset from all the sites except Gadanki (monthly values) are available on a daily scale and have been averaged to get the annual concentrations.

2.4 MERRA-2 data

Model simulated BC and OC columnar burden have been evaluated against MERRA-2 reanalysis data. MERRA-2 is an updated reanalysis of atmospheric data produced by the NASA Global Modeling and Assimilation Office (Buchard et al., 2017). MERRA-2 consists of parameters that are not available in its predecessor, MERRA. It includes updates of the Goddard Earth Observing System model and analysis scheme in order to give a more realistic view of the ongoing climate analysis beyond MERRA's jargon. This dataset addressed the limitations of MERRA. Various improvements in MERRA-2 include assimilation of aerosol observations and improved representation of stratosphere, including ozone and cryosphere. MERRA-2 data products are freely accessible through the NASA Goddard Earth Sciences Data Information Services Centre. We note that MERRA-2 data are also not observations and direct validation of the MERRA-2 columnar BC and OC burden is not possible.

2.5 MISR aerosol data

MISR on-board Terra satellite crosses the equator around 10:30 hrs local time. It has a high spatial resolution and a wide range of viewing angles. It views the Earth using four spectral bands in each of the nine cameras and has a weekly global coverage between ±82º. A detailed description is provided in the literature (Diner et al., 1998). MISR-AOD has a correlation coefficient of ~0.9 (for maritime sites) and ~0.7 (for dusty sites) w.r.t AERONET (Kahn et al., 2005). In the absence of any direct measurement, we use MISR fine AOD (AOD for particles smaller than 0.35 μm) as a proxy for anthropogenic AOD (Dey and Girolamo, 2010).

3. Results

3.1 Spatial distribution of carbonaceous aerosols

Figure 1 shows the spatial distributions of the annual surface concentration for BC and OC using the default and augmented model along with their differences. Several key features are notable. First, the OC concentration is almost three times higher than the BC concentration in the augmented model, consistent with the literature (Priyadharshini et al., 2019). Secondly, the concentrations are 2-3 times higher over the polluted IGP compared to the rest of India in the

https://doi.org/10.5194/gmd-2021-330
Preprint. Discussion started: 3 December 2021

augmented model. High aerosol loading over the IGP is a result of the combined effects of greater source strength, low topography surrounded by highlands to the north and south, and unfavourable meteorology (Dey and Girolamo, 2010; Srivastava et al., 2012). Thirdly, the BC and OC concentrations increase by >100% and >60%, respectively, over the IGP and by smaller margins elsewhere in the augmented model relative to the default configuration. The increase in the annual concentrations of surface BC and OC is mainly driven by the changes in the concentrations during the winter (JF), and pre-monsoon (MAM) seasons (Figure S2) since during the monsoon, precipitation removes large amounts of aerosols. The relative impact of the switch from the global to regional emission inventory (Figure S2) is greater than the impact of the implementation of the dynamic ageing scheme (Figure S1) on the observed increases in BC and OC mass concentrations in the augmented model.

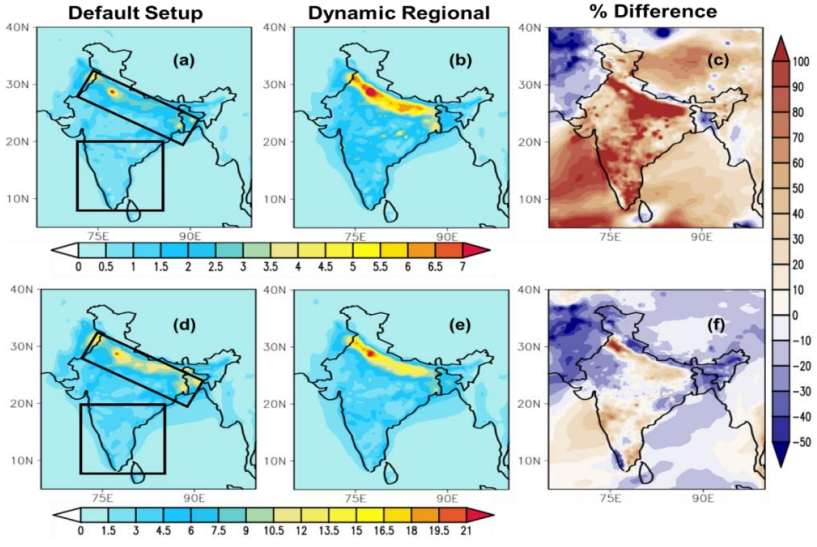

Figure 1. Spatial distribution of surface mass concentration (μg m^{-3}) of BC (a, b) and OC (d, e) in 2010 over the Indian subcontinent using (left) the default and (middle) the augmented model configurations. Figures 1c and 1f represent the corresponding percentage differences due to the augmented model set-up (positive values imply an increase in mass concentration). The vertical distributions (shown in Figure 3) are analysed for the IGP and PI sub-regions marked by boxes in the panels of the left column.

https://doi.org/10.5194/gmd-2021-330
Preprint. Discussion started: 3 December 2021

Geoscientific Model Development Discussions

We evaluate the performance of the customized model against BC surface concentrations measured at 24 sites across India (Figure S3). We note that the in-situ concentrations are point measurements while the model grids containing these sites are representative of 25 km by 25 km areas. The default model severely underestimates the surface BC compared to the in-situ observations (mean normalized bias, MNB = -69%). Previous model studies reveal that the BC concentration is underestimated almost 2-5 times across various sites in India (Nair et al., 2012; Ramachandran et al., 2021). Though the underestimation persists in the augmented model (by varying proportions across the sites), the simulated concentration magnitudes are closer to the observations (MNB = -51%), more so in the urban centres of the polluted IGP (e.g., Delhi, Kanpur, Varanasi, Kharagpur). In some cities (e.g., Dehradun, Dibrugarh, Ahmedabad) where the differences in global and regional emission inventories are small (Figure S1), the improvement in simulated BC concentrations is also limited. This suggests that the problem could be related to the emission fluxes. In several cities, especially in the North and South Indian regions (e.g., Goa, Nainital, Ooty, Thiruvananthapuram), the simulated BC using the augmented model shows an almost perfect match with the observations. Overall, the augmented model (R^2=0.66) performs better than the default model (R^2=0.6) in simulating surface BC concentrations, and the errors shown in Figure 2 could also be amplified by the fact that the model data refers to a 25 km × 25 km area as a single grid.

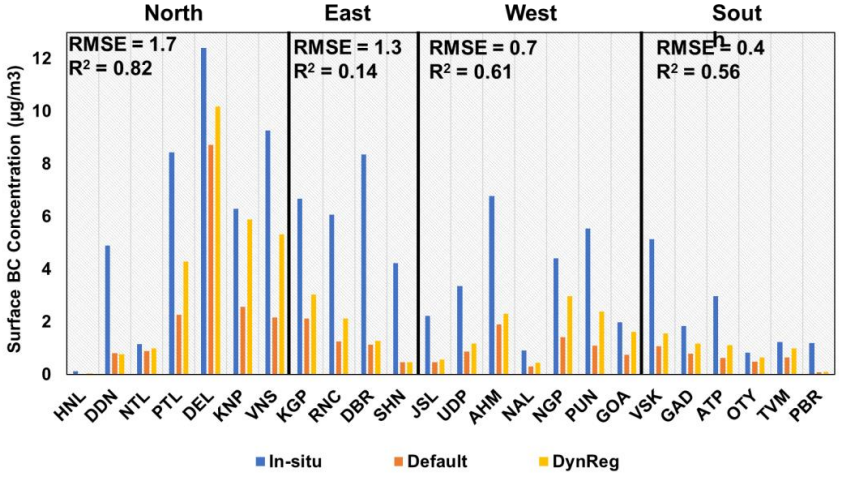

Figure 2. Comparison of simulated BC surface concentration (µg m^{-3}) using the default and augmented model with in-situ measurements from 24 cities across India. Locations of the cities

https://doi.org/10.5194/gmd-2021-330
Preprint. Discussion started: 3 December 2021


Geoscientific Model Development Discussions

are shown in Figure S2. RMSE (in μg m^{-3}) and R^2 between the customized model simulations and surface measurements are also provided.

Since there are no in-situ measurements of columnar burden available, we compare the simulated columnar burden (Figure 3) with data from Modern-Era Retrospective Analysis for Research and Applications, version 2 (MERRA-2) (Buchard et al., 2017). Similar to the surface mass concentration, the BC burden shows a more pronounced change than the OC burden due to the inclusion of the new model features. Though the simulated burden is still underestimated relative to the MERRA-2 data, the values in the augmented model are much closer to the reanalysis data. During the winter season (Jan-Feb), the percentage difference of model-simulated column burden (w.r.t. MERRA-2) decreases from >70% to ~ 35% for BC and from ~63% to ~49% for OC in the augmented model (Figures S4 and S5). A similar improvement is found in the pre-monsoon season (Mar-May). The higher loading results from higher magnitudes of regional emissions coupled with faster ageing and slower removal rate. The percentage difference increases for OC burden over northwest India, decreases over the IGP, and is negligible over the rest of the country. A probable explanation for such OC distribution relies on the emission inventories used since the OC emissions are slightly higher in the global inventory than those in the regional inventory over northwest India and lower in the IGP. Emissions over the PI are roughly similar in the two inventories (Figure S2). We also note that anthropogenic aerosol emissions vary on an annual basis in MERRA-2 (Buchard et al., 2017); hence, there could be larger uncertainties at a seasonal scale.

During the monsoon season (Jun-Sep), the BC loading increases in magnitude in the augmented model compared to the default set-up (Figure S4), mostly due to the implementation of the regional inventory. The magnitude of the simulated BC column burden is comparable between the Default_Sc and Dyn_sc experiments and between the Fix_Regio and Dyn_Regio (Figure S4), with an opposite pattern found for the OC column burden (Figure S5). Two possible reasons can explain this result. First, the OC emissions in the global inventory are higher than in the regional ones (Figure S1). Second, the model assumes that OC is 50% hydrophobic and 50% hydrophilic at the time of emission (for BC, it is 80% hydrophobic and 20% hydrophilic), and therefore the faster conversion to hydrophilic OC due to the dynamic ageing enhances the hydrophilic OC burden, which is subsequently removed by rain. In the post-monsoon season (Oct-Dec), an overall increase in column burden in the augmented model is observed throughout India. Higher emissions (in the case of the regional inventory) result in

https://doi.org/10.5194/gmd-2021-330
Preprint. Discussion started: 3 December 2021

higher concentrations of available condensing and coagulating particles, which in turn allows faster ageing of hydrophobic to hydrophilic BC leading to accumulation of BC particles in the atmosphere before their removal by dry deposition. The changes in the OC loading are negligible in this season.

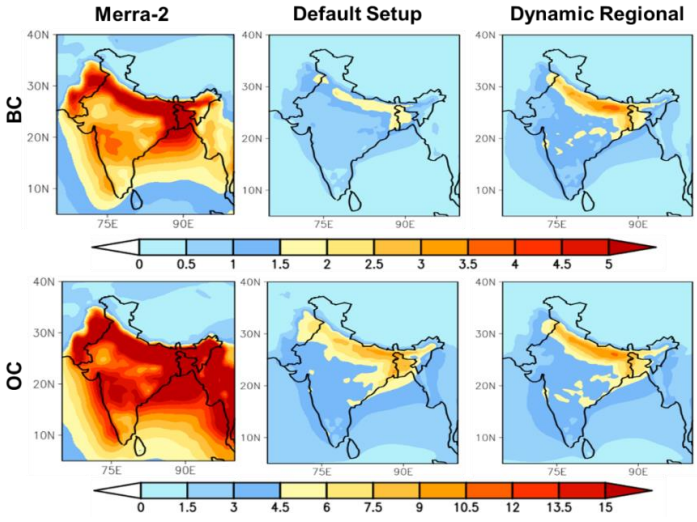

Figure 3. Comparison of spatial patterns of annual (top panel) BC and (bottom panel) OC column burden (mg m^{-2}).

3.2 Vertical distribution of carbonaceous aerosols

In this section, we analyse the effects of the model improvements on the vertical distribution of aerosols over the IGP and compare the results with the contrasting PI region, where the emissions are much lower. The two regions are indicated by the boxes in Figure 1 and Figure 4 longitude-altitude cross-sections of BC and OC mass concentration over the regions.

The vertically distributed mass concentrations of both BC and OC increase due to the model improvements up to 500 hPa. A larger increase is observed during the winter and post-monsoon seasons over the IGP (Figures S6 and S7). Both the BC and OC concentrations are comparable in the default and Dyn_global configurations, but they increase in the Fix_regio and Dyn_regio set-ups (Figures S6 and S7). While the role of emissions is only predominant during the post-

https://doi.org/10.5194/gmd-2021-330
Preprint. Discussion started: 3 December 2021

monsoon season, the highest increase due to the combined effect of the two improvements is observed during the winter. In these two seasons, the BC remains confined mostly within the lower troposphere while the OC is distributed up to the mid-tropospheric levels, which is indicative of higher concentrations of OC vertical transport than that of BC. During the pre-monsoon season, the vertical distributions of both BC and OC show responses similar to that of their spatial distributions. In the monsoon season, the tracer concentration is mainly confined to the surface levels, indicating a lower wet removal and slower ageing above 1000 hPa (Ghosh et al., 2021).

Over the PI, the concentrations of carbonaceous aerosols are lower than over the IGP, which limits the impact of dynamic ageing because of the lower availability of condensing and coagulating particles (relative to the IGP). This results in a slower ageing and lower accumulation of hydrophilic tracers in the troposphere. However, the vertical pumping effect is quite prominent during the winter season in the augmented configuration (Figures S6 and S7). During the pre-monsoon season, only the BC concentration shows an increment in the lower troposphere, while the OC concentration remains more or less unchanged. The PI receives rainfall during the southwest and northeast monsoon; hence the tracer concentration is further lowered during the monsoon and post-monsoon seasons.

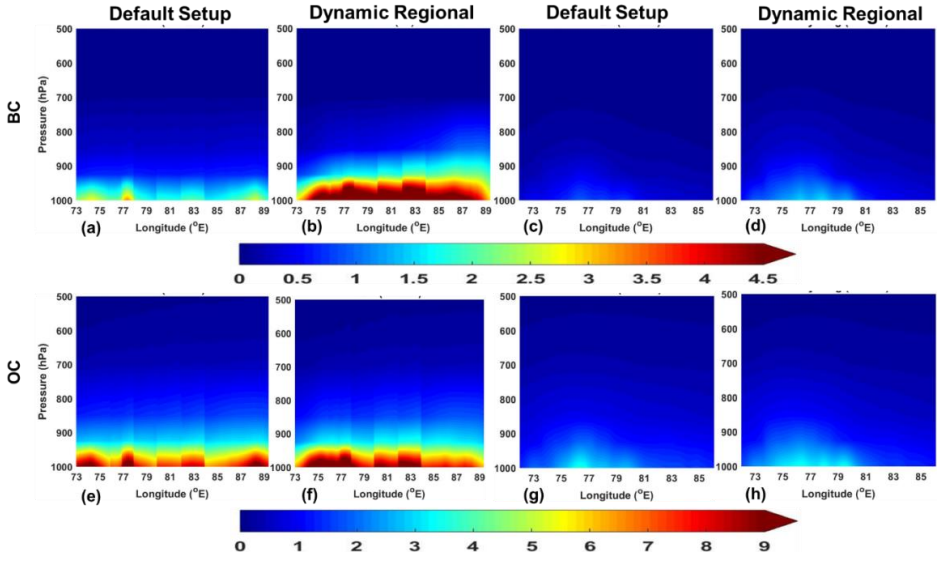

Figure 4. Longitude (in °E)-altitude (in hPa) cross-sections of (top panel) BC and (bottom panel) OC mass concentration (μg m^{-3}) over the IGP (a, b, e, f) and PI (c, d, g, h) for the default and customized model.

https://doi.org/10.5194/gmd-2021-330
Preprint. Discussion started: 3 December 2021

Geoscientific Model Development Discussions

3.3 Optical and radiative properties of anthropogenic aerosols

We now examine the effects of the model improvements on the optical properties of anthropogenic aerosols. In this regard, we note that the changes due to the implementation of the dynamic ageing scheme can alter only BC and OC concentrations, while the changes related to the emission inventory impact the sulphate concentration as well. We consider the AOD due to small particles (radius<0.35 μm) from MISR (Kahn and Gaitley, 2015), as a proxy for anthropogenic AOD (hereafter AAOD) since direct measurement of AAOD are not available to evaluate our model performance (Figure 5).

The simulated annual AAOD is >50% lower than the MISR small-AOD over the polluted IGP and 30-50% lower over the PI in the default model. This is consistent with the previous studies (Nair et al., 2012). These model underestimations improve by 25-35% over the IGP and parts of PI in the augmented model. The seasonal plots (Figure S8) clearly show an increase of AAOD in all seasons except during the monsoon. This increase in AAOD is due to both the implementation of region-specific emission fluxes and the dynamic ageing scheme. The AAOD still remains underestimated in some regions, which can possibly be addressed by further improvements of the emission estimates, for example, the addition of missing sectors (e.g., crematorium, municipal solid waste burning, etc.), improving sectoral methodologies for informal activities and incorporation of regionally measured emission factors.

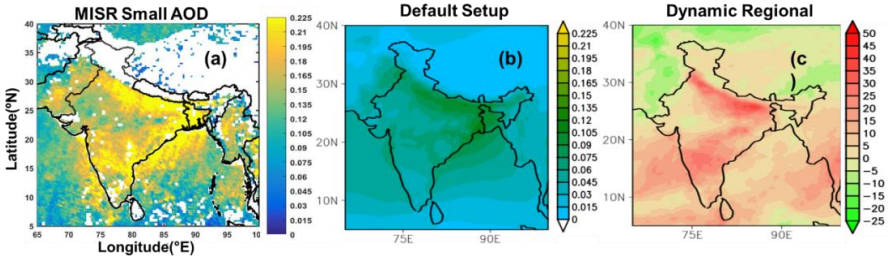

Figure 5. Spatial distribution of (a) MISR small mode AOD ('white' color implies 'no data'), (b) AAOD simulated by default_sc, and (c) percentage increase in AAOD simulated by the augmented model w.r.t default_sc for 2010.

Spatial patterns of the annual top-of-the-atmosphere (TOA), surface, and atmospheric radiative forcing associated with the anthropogenic aerosols for the augmented model are shown in Figure 6. The TOA aerosol radiative forcing lies in the range -0.5 to -1.5 W m^{-2} over most of the Indian landmass, except the IGP, where it is positive (0.25 to 1 W m^{-2}) due to the

https://doi.org/10.5194/gmd-2021-330
Preprint. Discussion started: 3 December 2021

higher concentration of carbonaceous aerosols (Figure 3), particularly BC. The TOA forcing is also positive over the Indian desert and snow-covered regions even when the carbonaceous aerosol concentrations are lower or comparable to the rest of India. The high surface albedo in these regions allows for an enhanced interaction of the carbonaceous aerosols with solar radiation, resulting in a warming effect (Ramachandran and Kedia, 2010). The surface radiative forcing is found to be larger than -10 W m^{-2} over the polluted IGP, which is consistent with published results (Ramanathan and Carmichael, 2008). Over the rest of India, the surface forcing values lie between -3 to -8 W m^{-2}. Due to the model improvements (forcing estimates with the default model are shown in Figure S8), the TOA forcing changes by -72.75%, and the surface dimming increases by 39.73% over the IGP and by -23.94% and 34.35%, respectively, over PI. As a result, the atmospheric heating increases by ~9 W m^{-2} over the IGP. The simulated surface shortwave radiation shows a statistically significant ($p<0.05$) correlation with the observations from CERES (Su et al., 2005) all-sky and clear-sky radiation throughout the year except in MAM and JJAS clear-sky conditions (Figure S9 and S10).

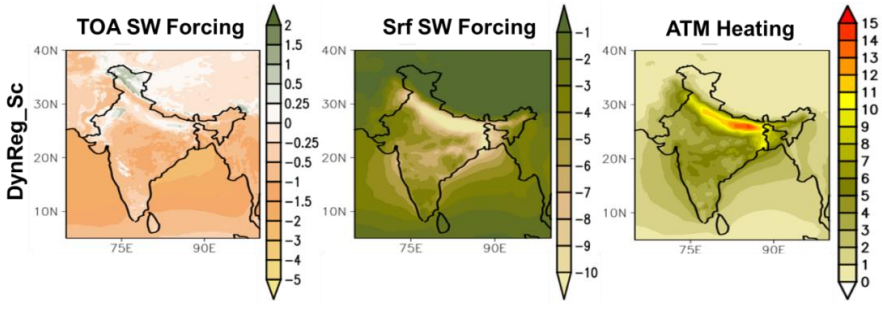

Figure 6. Annual variation of SW radiative forcing (W/m^2) at TOA (left column), at the surface (middle column), and the resultant atmospheric heating (W/m^2) (right column) for the customized set-up.

4. Discussion and conclusions

Accurate estimates of emission fluxes and a better representation of aerosol processes are required to improve the representation of aerosol life-cycle and radiative effects in climate models. Here we augmented the regional climate model RegCM4 by implementing a dynamic ageing scheme and a regional emission inventory and examined the combined impact of these factors on the model performance over the Indian monsoon region. We note that though the

https://doi.org/10.5194/gmd-2021-330
Preprint. Discussion started: 3 December 2021

aerosol simulations improve due to these model enhancements, some systematic biases persist (underestimation of carbonaceous aerosol concentrations) and need to be further addressed. For example, RegCM has a bulk scheme for anthropogenic aerosols, and thus the number concentration is calculated from the bulk mass concentration (Ghosh et al. 2021). The anthropogenic aerosol module can thus be improved by including a particle size-dependent representation. In addition, the present dynamic ageing timescale depends only on the anthropogenic aerosol number concentration, while it should, in fact, depend on the total (anthropogenic + natural) number concentrations. The simulations presented in this work did not include natural aerosols, which could have impacted the meteorology through dynamic feedbacks, possibly affecting the carbonaceous aerosol burden. This aspect will be examined in future work. Thirdly, though the emission fluxes of BC, OC, and SO_2 are higher in the region than the global inventory, there may still be uncertainty related to missing sectoral sources.

Our work demonstrates that even the improvement of some aspects of the aerosol representation can lead to substantial enhancements in the model performance. We also find that over the South Asian monsoon region, particularly over highly polluted regions such as the IGP, the default model significantly underestimates the surface dimming and atmospheric heating, which can have implications for climate studies (Das et al., 2016, 2020) and this problem is substantially ameliorated with our model augmentations.

The key conclusions of our work can be summarized as follows.

1. The conclusion in the model RegCM4 of a dynamic ageing scheme and a regional emission inventory substantially improves the model performance over the Indian sub-continent.
2. The BC and OC surface concentration and column burden increase due to the model improvements, more so as a combined effect of the two factors than because of the individual ones.
3. The TOA, surface, and atmospheric radiative forcing are estimated to be -0.3, -5.3, and 5.0 W m^{-2}, respectively, over the polluted IGP using the augmented model, but they could still be underestimated.

Data availability. The model RegCM4.6 code is freely available online from https://zenodo.org/record/5729783#.YaDifbso-Uk. The anthropogenic aerosol emissions considered for the simulations are taken from the IIASA inventory. The data used can be easily accessed online http://climadods.ictp.it/Data/RegCM_Data/RCP_EMGLOB_PROCESSED/iiasa/

https://doi.org/10.5194/gmd-2021-330
Preprint. Discussion started: 3 December 2021

website. Input files for the RegCM4 model are archived in http://clima-dods.ictp.it/Data/RegCM_Data/ website. MISR data is available freely from https://www-misr.jpl.nasa.gov/ while MERRA-2 data is freely available from the NASA Giovanni site https://giovanni.gsfc.nasa.gov/giovanni/ .

Author contributions.

SG and SD (corresponding author) planned the experiments and wrote the first draft. SG carried out the simulations and data analysis with SD, SD (third author), NR, and GG. CV provided the regional emission inventory. DG and FG provided inputs on experiment design. SNT, SR, TAR, HG, and AKS provided the BC data for evaluation. All authors contributed and edited the manuscript.

Competing Interests. All the authors declare that they have no conflict of interest.

Acknowledgements. We thank the Aerosol Radiative Forcing over India (ARFINET) project of ISRO GBP for sharing the BC data. The authors thank the internal review committee of the NCAP-COALESCE project for their comments and suggestions. The views expressed in this document are solely those of the authors and do not necessarily reflect those of the Ministry. The Ministry does not endorse any products or commercial services mentioned in this publication. SG acknowledges the supercomputing facility Keeling of the University of Illinois Urbana-Champaign.

Financial Support. This work is supported by the MoEFCC under the NCAP-COALESCE project [Grant 14/10/2014-CC(Vol II)]. SG acknowledges the support for the DST-INSPIRE fellowship, Fulbright-Kalam Climate Fellowship. SD acknowledges IIT Delhi for the support of the Institute Chair. NR acknowledges funding from NSF AGS-1254428 and DOE grant DE-SC0019192.

References

1. Ajay, P., Pathak, B., Solmon, F., Bhuyan, P. K., Giorgi, F.: Obtaining best parameterization scheme of RegCM 4.4 for aerosols and chemistry simulations over the CORDEX South Asia. Clim Dyn 53, 329–352, https://doi.org/10.1007/s00382-018-4587-3, 2019.
2. Babu, S. S., Manoj, M. R., Krishna Moorthy, K., Gogoi, M. M., Nair, V. S., Kompalli, S.K., Satheesh, S. K., Niranjan, K., Ramagopal, K., Bhuyan, P. K., and Singh, D.:

https://doi.org/10.5194/gmd-2021-330
Preprint. Discussion started: 3 December 2021


Geoscientific Model Development Discussions

457 Trends in aerosol optical depth over Indian region: Potential causes and impact
458 indicators, J. Geophys. Res. Atmos. 118, 11794– 11806,
459 https://doi.org/10.1002/2013JD020507, 2013.
460 3. Bond, T. C., et al.: Bounding the role of black carbon in the climate system: A scientific
461 assessment, J. Geophys. Res. Atmos., 118, 5380– 5552,
462 https://doi.org/10.1002/jgrd.50171, 2013.
463 4. Bretherton C.S., McCaa, J.R. and Grenier, H. A new parameterization for shallow
464 cumulus convection and its application to marine subtropical cloud-topped boundary
465 layers. I. Description and 1D results. Mon Weather Rev 132, 864–882,
466 https://doi.org/10.1175/1520-0493(2004)132<0864:ANPFSC>2.0.CO;2, 2004.
467 5. Buchard, V., Randles, C. A., da Silva, A. M., Darmenov, A., Colarco, P. R.,
468 Govindaraju, R., Ferrare, R., Hair, J., Beyersdorf, A. J., Ziemba, L. D., and Yu, H.: The
469 MERRA-2 Aerosol Reanalysis, 1980 Onward. Part II: Evaluation and Case Studies,
470 Journal of Climate 30(17), 6851-6872, https://doi.org/10.1175/JCLI-D-16-0613.1,
471 2017.
472 6. Das, S., Dey, S., Dash, S. K., Giuliani, G., and Solmon, F.: Dust aerosol feedback on
473 the Indian summer monsoon: Sensitivity to absorption property. J. Geophys. Res.
474 Atmos. 120, 9642–9652, https://doi.org/10.1002/2015JD023589, 2015.
475 7. Das, S., Dey, S., and Dash, S. K.: Direct radiative effects of anthropogenic aerosols on
476 Indian summer monsoon circulation, Theor Appl Climatol. 124, 629–639,
477 https://doi.org/10.1007/s00704-015-1444-8, 2016.
478 8. Das, S., Giorgi, F., Giuliani, G., Dey, S., and Coppola, E.: Near-future anthropogenic
479 aerosol emission scenarios and their direct radiative effects on the present-day
480 characteristics of the Indian summer monsoon, Journal of Geophysical Research:
481 Atmospheres 125, e2019JD031414, https://doi.org/10.1029/2019JD031414, 2020.
482 9. Dash, S. K., Shekhar, M. S. and Singh G. P.: Simulation of Indian summer monsoon
483 circulation and rainfall using RegCM3, Theor. Appl. Climatol. 86, 161–172,
484 https://doi.org/10.1007/s00704-006-0204-1, 2006.
485 10. Dee, D.P., Uppala, S.M., Simmons, A.J., Berrisford, P., Poli, P., Kobayashi, S., Andrae,
486 U., Balmaseda, M.A., Balsamo, G., Bauer, P., Bechtold, P., Beljaars, A.C.M., van de
487 Berg, L., Bidlot, J., Bormann, N., Delsol, C., Dragani, R., Fuentes, M., Geer, A.J.,
488 Haimberger, L., Healy, S.B., Hersbach, H., Hólm, E.V., Isaksen, L., Kållberg, P.,
489 Köhler, M., Matricardi, M., McNally, A.P., Monge-Sanz, B.M., Morcrette, J.-J., Park,
490 B.-K., Peubey, C., de Rosnay, P., Tavolato, C., Thépaut, J.-N. and Vitart, F.: The ERA-

https://doi.org/10.5194/gmd-2021-330
Preprint. Discussion started: 3 December 2021

Interim reanalysis: configuration and performance of the data assimilation system, Q.J.R. Meteorol. Soc. 137, 553-597, https://doi.org/10.1002/qj.828, 2011.

11. Dey, S., and Di Girolamo, L.: A climatology of aerosol optical and microphysical properties over the Indian subcontinent from 9 years (2000–2008) of Multiangle Imaging Spectroradiometer (MISR) data, J. Geophys. Res. 115, D15204, https://doi.org/10.1029/2009JD013395, 2010.
12. Dickinson, R.E., Sellers, H.A. and Kennedy, P.J.: Biosphere atmosphere transfer scheme (BATS) version 1E as coupled to the NCAR community climate model, Technical note NCAR/TN-3871 STR, p 72, DOI:10.5065/D67W6959, 1993.
13. Diner, D. J., Beckert, J.C., Reilly, T.H., Bruegge, C.J., Conel, J. E., Kahn, R., Martonchik, J.V., Ackerman, T.P., Davies, R., Gerstl, S.A.W., Gordon, H.R., Muller, J-P., Myneni, R.B., Sellers, R.J., Pinty, B., and Verstraete, M.M.: Multi-angle Imaging Spectro Radiometer (MISR) instrument description and experiment overview, IEEE Transactions on Geoscience and Remote Sensing, 36 (4), 1072-1087, DOI: 10.1109/36.700992, 1998.
14. Emanuel, K.A. and Rothman, M.Z.: Development and evaluation of a convection scheme for use in climate models, J. Atmos. Sci. 56, 1766–1782, https://doi.org/10.1175/1520-0469(1999)056<1766:DAEOAC>2.0.CO;2, 1999.
15. Fierce, L., Riemer, N., and Bond, T.: Toward Reduced Representation of Mixing State for Simulating Aerosol Effects on Climate, Bull. Amer. Meteor. Soc., 98, 971–980, DOI: 10.1175/BAMS-D-16-0028.1, 2016.
16. Gadhavi, H. S., Renuka, K., Kiran, V. R., Jayaraman, A., Stohl, A., Klimont, Z., and Beig, G. Evaluation of black carbon emission inventories using a Lagrangian dispersion model - a case study over southern India, Atmospheric Chemistry and Physics, 15(3), 1447–1461, https://doi.org/10.5194/acp-15-1447-2015, 2015.
17. Ghosh, S., Riemer, N., Giuliani, G., Giorgi, F., Ganguly, D., and Dey, S.: Sensitivity of carbonaceous aerosol properties to the implementation of a dynamic ageing parameterization in the regional climate model RegCM, Journal of Geophysical Research: Atmospheres, 126, e2020JD033613, https://doi.org/10.1029/2020JD033613, 2021.
18. Giorgi, F., Jones, C. and Asrar, G. R.: Addressing climate information needs at the regional level: the CORDEX framework, WMO Bulletin 58(3), 175-183, 2009.
19. Giorgi, F., Coppola, E., Solmon, F., Mariotti, L., Sylla, M. B., Bi, X., Elguindi, N., Diro, G. T., Nair, V., Giuliani, G., Turuncoglu, U. U., Cozzini, S., Güttler, I., O'Brien,

https://doi.org/10.5194/gmd-2021-330
Preprint. Discussion started: 3 December 2021

T. A., Tawfik, A. B., Shalaby, A., Zakey, A. S., Steiner, A. L., Stordal, F., Sloan, L. C., and Brankovic, C.: RegCM4: model description and preliminary tests over multiple CORDEX domains, Clim. Res. 52, 7-29, https://doi.org/10.3354/cr01018, 2012.

20. Gogoi et al., Response of ambient BC concentration across the Indian region to the nation-wide lockdown: results from the ARFINET measurements of ISRO-GBP, Current Science 120(2), 341-351, https://doi.org/10.18520/cs%2Fv120%2Fi2%2F341-351, 2021.
21. Grell, G. A.: Prognostic Evaluation of Assumptions Used by Cumulus Parameterizations, Monthly Weather Review 121(3), 764-787, https://doi.org/10.1175/1520-0493(1993)121<0764:PEOAUB>2.0.CO;2, 1993.
22. Grenier, H. and Bretherton, C.S. A moist PBL parameterization for large-scale models and its application to subtropical cloud-topped marine boundary layers, Mon. Weather Rev., 129, 357–377, https://doi.org/10.1175/1520-0493(2001)129<0357:AMPPFL>2.0.CO;2, 2001.
23. Hansen, A.D.A., Rosen, H. and Novakov, T.: The Aethalometer—An Instrument for the Real-Time Measurement of Optical Absorption by Aerosol Particles, Science of The Total Environment, 36, 191-196, 10.1016/0048-9697(84)90265-1, 1984.
24. Jain, C. D., Gadhavi, H. S., Wankhede, T., Kallelapu, K., Sudhesh, S., Das, L. N., Pai, R. U., and Jayaraman, A.: Spectral Properties of Black Carbon Produced during Biomass Burning, Aerosol and Air Quality Research, 18(3), 671–679, doi: 10.4209/aaqr.2017.03.0102, 2018.
25. Kahn, R., Li, W., Martonchik, J. V., Bruegge, C. J., Diner, D. J., Gaitley, B. J., Abdou, W., Dubovik, O., Holben, B., Smirnov, A., Jin, Z., & Clark, D.: MISR calibration and implications for low-light-level aerosol retrieval over dark water, J. Atmos. Sci. 62 (4), 1032-1052, https://doi.org/10.1175/JAS3390.1, 2005.
26. Kahn, R. A., and Gaitley, B. J.: An analysis of global aerosol type as retrieved by MISR, J. Geophys. Res. Atmos. 120, 4248– 4281, https://doi.org/10.1002/2015JD023322, 2015.
27. Kanakidou, M., Seinfeld, J. H., Pandis, S. N., Barnes, I., Dentener, F. J., Facchini, M. C., Van Dingenen, R., Ervens, B., Nenes, A., Nielsen, C. J., Swietlicki, E., Putaud, J. P., Balkanski, Y., Fuzzi, S., Horth, J., Moortgat, G. K., Winterhalter, R., Myhre, C. E. L., Tsigaridis, K., Vignati, E., Stephanou, E. G., and Wilson, J.: Organic aerosol, and global climate modelling: A review, Atmos. Chem. Phys. 5, 1053–1123, https://doi.org/10.5194/acp-5-1053-2005, 2005.

https://doi.org/10.5194/gmd-2021-330
Preprint. Discussion started: 3 December 2021


Geoscientific Model Development Discussions

559 28. Kiehl, J.T., Hack, J. J., Bonan, G. B., Boville, B. A., Briegleb, B. P., Williamson, D.
560 L., & Rasch, P. J.: Description of the NCAR community climate model (CCM3), Tech.
561 Rep. National Center for Atmospheric Research, NCAR/TN-420+STR, P 152,
562 doi:10.5065/D6FF3Q99, 1996.
563 29. Nair, V.S., Solmon, F., Giorgi, F., Mariotti, L., Babu, S.S. and Moorthy, K. K.
564 Simulation of South Asian aerosols for regional climate studies, J Geophys Res. 117,
565 D04209, https://doi.org/10.1029/2011JD016711, 2012.
566 30. O'Brien, T.A., Chuang, P.Y., Sloan, L.C., Faloona, I.C. and Rossiter, D.L.: Coupling a
567 new turbulence parametrization to RegCM adds realistic stratocumulus clouds, Geosci.
568 Mod. Dev. 5, 989–1008, https://doi.org/10.5194/gmd-5-989-2012, 2012.
569 31. Pal, J. S., Small, E. E. and Eltahir E. A. B.: Simulation of regional-scale water and
570 energy budgets: Representation of subgrid cloud and precipitation processes within
571 RegCM, J. Geophys. Res. 105(D24), 29579–29594,
572 https://doi.org/10.1029/2000JD900415, 2000.
573 32. Pattnayak, K.C, Panda, S.K., Saraswat, V. and Dash, S. K.: Assessment of two versions
574 of a regional climate model in simulating the Indian Summer Monsoon over South Asia
575 CORDEX domain, Clim Dyn 50, 3049–3061, https://doi.org/10.1007/s00382-017-
576 3792-9, 2018.
577 33. Priyadharshini, B., Verma, S., Chatterjee, A., Kumar Sharma S. and Kumar Mandal,
578 T.: Chemical Characterization of Fine Atmospheric Particles of Water-Soluble Ions and
579 Carbonaceous Species in a Tropical Urban Atmosphere over the Eastern Indo-Gangetic
580 Plain, Aerosol and Air Quality Research 19, 129–147,
581 https://doi.org/10.4209/aaqr.2017.12.0606, 2019.
582 34. Putaud, J.P., Van Dingenen, R. , Alastuey, A., Bauer, H., Birmili, W., Cyrys, J., Flentje,
583 H., Fuzzi, S., Gehrig, R., Hansson, H.C., Harrison, R.M., Herrmann, H., Hitzenberger,
584 R., Hüglin, C., Jones, A.M., Kasper-Giebl, A., Kiss, G., Kousa, A. , Kuhlbusch, T.A.J.,
585 Löschau, G., Maenhaut, W., Molnar, A., Moreno, T., Pekkanen, J., Perrino, C., Pitz,
586 M., Puxbaum, H., Querol, X., Rodriguez, S., Salma, I., Schwarz, J., Smolik, J.,
587 Schneider, J., Spindler, G., ten Brink, H., Tursic, J., Viana, M., Wiedensohler, A., Raes,
588 F.: A European aerosol phenomenology-3: Physical and chemical characteristics of
589 particulate matter from 60 rural, urban, and kerbside sites across Europe, Atmos.
590 Environ. 44, 1308–1320, https://doi.org/10.1016/j.atmosenv.2009.12.011, 2010.

https://doi.org/10.5194/gmd-2021-330
Preprint. Discussion started: 3 December 2021

591 35. Qian, Y., Giorgi, F., Huang, Y., Chameides, W. L. and Luo, C.: Simulation of
592 anthropogenic sulfur over East Asia with a regional coupled chemistry-climate model,
593 Tellus, Ser. B. 53, 171–191, https://doi.org/10.3402/tellusb.v53i2.16573, 2001.
594 36. Rai, P. K., Singh, G. P. and Dash, S. K.: Projected Change and Variability Assessment
595 of Indian Summer Monsoon Precipitation in South Asia CORDEX Domain Under
596 High-Emission Pathway, Pure Appl. Geophys. 177(7), 3475–3499,
597 https://doi.org/10.1007/s00024-019-02373-3, 2019.
598 37. Ramachandran, S., and Kedia, S.: Black carbon aerosols over an urban region:
599 Radiative forcing and climate impact, J. Geophys. Res., 115, D10202,
600 doi:10.1029/2009JD013560, 2010 .
601 38. Ramachandran, S., Rajesh, T.A. and R. Cherian, R.: Black carbon aerosols over source
602 vs. background region: Atmospheric boundary layer influence, potential source regions,
603 and model comparison, Atmospheric Research, 256, 105573, ISSN 0169-8095,
604 https://doi.org/10.1016/j.atmosres.2021.105573, 2021.
605 39. Ramanathan, V. and Carmichael G.: Global and regional climate changes due to black
606 carbon. Nat Geos. 1, 221-227, https://doi.org/10.1038/ngeo156, 2008.
607 40. Riemer, N., West, M., Zaveri, R. A., and Easter, R. C.: Simulating the evolution of soot
608 mixing state with a particle resolved aerosol model, J. Geophys. Res., 114, D09202,
609 doi:10.1029/2008JD011073, 2009.
610 41. Riemer, N., Ault, A. P., West, M., Craig, R. L., & Curtis, J. H.: Aerosol mixing state:
611 Measurements, modeling, and impacts, Reviews of Geophysics 57, 187– 249,
612 https://doi.org/10.1029/2018RG000615, 2019.
613 42. Satheesh, S.K.: Aerosol radiative forcing over land: effect of surface and cloud
614 reflection, Ann. Geophys. 20, 2105–2109, https://doi.org/10.5194/angeo-20-2105-
615 2002, 2002.
616 43. Shalaby, A., Zakey, A. S., Tawfik, A. B., Solmon, F., Giorgi, F., Stordal, F., Sillman,
617 S., Zaveri, R. A., and Steiner, A. L.: Implementation and evaluation of online gas-phase
618 chemistry within a regional climate model (RegCM-CHEM4), Geosci. Model Dev., 5,
619 741–760, https://doi.org/10.5194/gmd-5-741-2012, 2012.
620 44. Singh, A., Rastogi, N., Kumar, V., Slowik, J. G., Satish, R., Lalchandani, V., Thamban,
621 N. M., Rai, P., Bhattu, D., Vats, P., Ganguly, D., Tripathi, S.N., and Prévôt, André S.H.:
622 Sources and characteristics of light-absorbing fine particulates over Delhi through the
623 synergy of real-time optical and chemical measurements, Atmos. Environ. 252,
624 118338, https://doi.org/10.1016/j.atmosenv.2021.118338, 2021.

https://doi.org/10.5194/gmd-2021-330
Preprint. Discussion started: 3 December 2021


Geoscientific Model Development Discussions

625 45. Solmon, F., Giorgi, F. and Liousse, C. Aerosol modelling for regional climate studies:
626 application to anthropogenic particles and evaluation over a European/African
627 domain, Tellus B 58, 51–72, https://doi.org/10.1111/j.1600-0889.2005.00155.x, 2006.
628 46. Srivastava, A. K., Dey, S., and Tripathi, S. N. Aerosol characteristics over the Indo-
629 Gangetic Basin: Implications to regional climate, Atmospheric Aerosols-Regional
630 Characteristics-Chemistry and Physics 10, 47782, DOI: 10.5772/47782, 2012.
631 47. Su, W., Charlock, T. P. and Rose, F. G.: Deriving surface ultraviolet radiation from
632 CERES surface and atmospheric radiation budget: Methodology, J. Geophys. Res. 110
633 (D14209), https://doi.org/10.1029/2005JD005794, 2005.
634 48. Tibrewal, K. and Venkataraman, C.: Climate co-benefits of air quality and clean energy
635 policy in India, Nat Sustain. 4, 305–313, https://doi.org/10.1038/s41893-020-00666-3,
636 2021.
637 49. Tiedtke, M.: A comprehensive mass-flux scheme for cumulus parameterization in
638 large-scale models, Mon. Weather Rev. 117, 1779–1800, https://doi.org/10.1175/1520-
639 0493(1989)117<1779:ACMFSF>2.0.CO;2, 1989.
640 50. Tripathi, S. N., Dey, S., Tare, V., Satheesh, S. K., Lal, S., and Venkataramani, S.:
641 Enhanced layer of black carbon in a north Indian industrial city, Geophys. Res. Lett.,
642 32, L12802, https://doi.org/10.1029/2005GL022564, 2005.
643 51. UNFCC Report 2015
644 52. Venkataraman, C., Brauer, M., Tibrewal, K., Sadavarte, P., Ma, Q., Cohen, A.,
645 Chaliyakunnel, S., Frostad, J., Klimont, Z., Martin, R. V., Millet, D. B., Philip, S.,
646 Walker, K., and Wang, S.: Source influence on emission pathways and ambient PM2.5
647 pollution over India (2015-2050), Atmos. Chem. Phys. 18, 8017-8039,
648 https://doi.org/10.5194/acp-18-8017-2018, 2018.
649 53. Venkataraman, C., Bhushan, M., Dey, S., Ganguly, D., Gupta, T., Habib, G., Kesarkar,
650 A., Phuleria, H., & Raman, R. S.: Indian Network Project on Carbonaceous Aerosol
651 Emissions, Source Apportionment and Climate Impacts (COALESCE), Bulletin of the
652 American Meteorological Society, 101(7), E1052-E1068,
653 https://doi.org/10.1175/BAMS-D-19-0030.1, 2020.
654 54. Zakey, A. S., Solmon, F. and Giorgi, F.: Development and testing of a desert dust
655 module in a regional climate model, Atmos. Chem. Phys. 6, 4687–4704,
656 https://doi.org/10.5194/acp-6-4687-2006, 2006.

https://doi.org/10.5194/gmd-2021-330
Preprint. Discussion started: 3 December 2021

55. Zakey, A. S., Giorgi, F. and Bi, X.: Modeling of sea salt in a regional climate model: Fluxes and radiative forcing, J. Geophys. Res. 113, D14221, https://doi.org/10.1029/2007JD009209, 2008.

56. Zaveri, R. A., Easter, R. C., Fast, J. D., and Peters, L. K.: Model for Simulating Aerosol Interactions and Chemistry (MOSAIC), J. Geophys. Res., 113, D13204, doi:10.1029/2007JD008782, 2008.